Open File

Open File

UNITED STATES
DEPARTMENT OF THE INTERIOR
GEOLOGICAL SURVEY

Mail Stop 964, Federal Center, Box 25046
Denver, Colorado 80225

Rock property analysis of core samples from the Yucca Mountain UE25a-1 borehole, Nevada Test Site, Nevada

by

Lennart A. Anderson

Open-File Report 81-1338

1981

Prepared by the U.S. Geological Survey

for

Nevada Operations Office
U.S. Department of Energy
(Memorandum of Understanding EW-78-A-08-1543)

CONTENTS

ILLUSTRATIONS

ILLUSTRATIONS--Continued

TABLES

ERRATA SHEET

Figure 2, page 5 - 0.2M KCL-silica gel should read: gel made from fumed quartz and 0.2M KCL solution.

Figure 4, page 10 - TEFLON should read: Vinyl

Rock property analysis of core samples from the Yucca Mountain UE25a-1 borehole, Nevada Test Site, Nevada

by

Lennart A. Anderson

ABSTRACT

Core samples from the Yucca Mountain UE25a-1 borehole were measured for bulk density, porosity, resistivity, induced polarization, compressional sonic velocity, hydraulic conductivity (water permeability), magnetic susceptibility, and remanent magnetization as part of a large-scale site evaluation program designed to identify suitable locations for the containment of radioactive waste products. The samples are representative of stratigraphic units of the Paintbrush Tuff, the tuffaceous beds of Calico Hills, and the Crater Flat Tuff. Resistivity and bulk density values of water-saturated samples closely approximate those at near in situ levels of water saturation and variations in resistivity, density, and sonic velocity are largely dependent upon porosity. The Tiva Canyon Member of the Paintbrush Tuff has an inversely polarized component of remanent magnetization and the entire Paintbrush has a magnetization appreciably greater than the underlying formations. There is no direct correlation between porosity and permeability; the latter varying widely and often decreasing with time as unconsolidated particles within the pore network are repositioned so as to impede the continued flow of water through the rock.

Introduction

Fifty-nine core samples from the Yucca Mountain UE25a-1 borehole on the Nevada Test Site (NTS) were obtained for selected rock property measurements as part of a large-scale site evaluation program designed to identify suitable underground repositories for radioactive waste products. Yucca Mountain lies in the southwest sector of NTS within the Topopah Spring SW Quadrangle (figure 1).

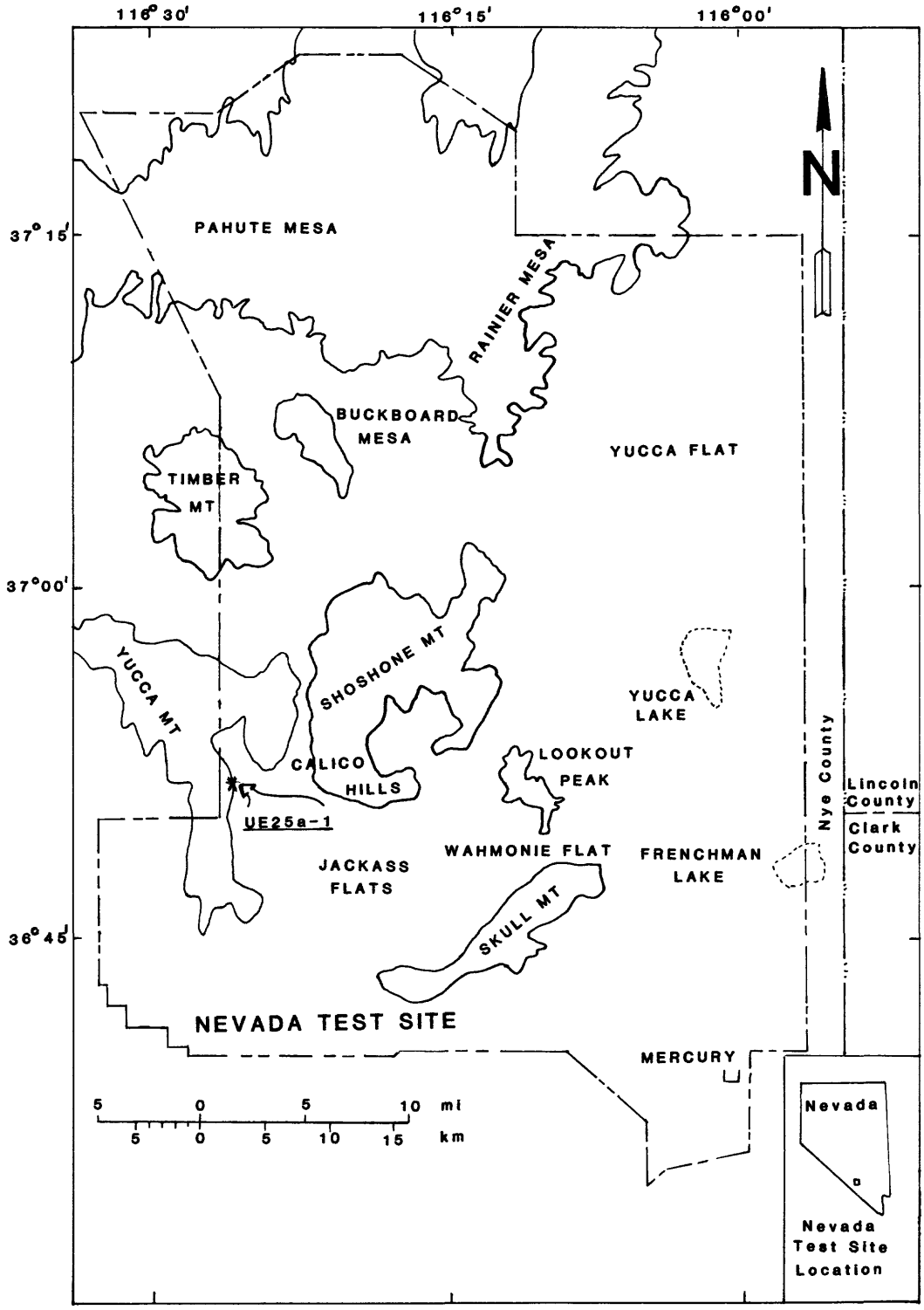

Figure 1- Map of the Nevada Test Site showing the location of the Yucca Mountain UE25a-1 borehole.

The borehole was drilled to a depth of 762 meters (2500 feet) penetrating the Tiva Canyon and Topopah Spring Members of the Paintbrush Tuff, the tuffaceous beds of Calico Hills, and the Prow Pass and Bullfrog Members of the Crater Flat Tuff. The rocks, Miocene in age, are described by Spengler and others (1979) as primarily nonwelded to densely welded ash-flow and bedded tuffs. In a subsequent paper Spengler and Rosenbaum (1980) report that a 6.7 meter (22 feet) section of the Pah Canyon Member of the Paintbrush Tuff has been identified within the bedded tuffs overlying the Topopah Spring Member.

Core samples were selected at the drill site so as to be representative of the major lithologic variations observed within the principal stratigraphic units. Following delivery to the Denver laboratories of the USGS, the samples were measured for electrical resistivity, induced polarization, porosity, bulk-density, compressional sonic velocity, hydraulic conductivity (water permeability), remanent magnetization, and magnetic susceptibility. The results of the measurements are intended for use in the interpretation of inhole and surface geophysical surveys as well as to provide a means for rock property characterization that is not normally possible with conventional borehole techniques.

Laboratory procedures for sample measurements

Upon extraction from the borehole, the cores were washed free of drilling mud, labeled as to depth and vertical attitude, wrapped in aluminum foil, and coated with beeswax in an effort to minimize the loss of natural pore water during the interim period prior to rock property analysis. To test the effectiveness of the preservation technique, the cores were cut into lengths approximately equal to their diameters and then measured for resistivity and bulk density. These measurements were repeated following drying and resaturation with tap water and compared with the initial measurements as a means of estimating the level of water retentivity in the natural state core.

Electrical resistivity measurements at a frequency of 100 Hz were made using a four-terminal sample holder and a Hewlett-Packard LCR meter, model 4262A. The sample holder is of simple design consisting of current and potential electrodes held apart from the core sample by a gel made from fumed Cab-O-Sil silica and a 0.2M solution of potassium chloride whose principal purpose is to provide for current flow through the rock. A resistance value (R) is read directly from the meter and resistivity is computed by use of the formula

$$\rho = \frac{RA}{\ell} \qquad (1)$$

where A and ℓ are the calipered measurements of length and cross-sectional area, respectively.

Direct current resistivity and induced polarization (IP) data were acquired with a Huntec Mark III receiver and a custom-built transmitter (figure 2). Using the same sample holder as used with the 100 Hz resisitivity measurements the transmitted signal was passed through a current-controlling device which limited the density of current flow through the rock to less than 1×10^{-5} amps/cm^2. This was done to avoid the non-linear effects in the IP response inherent in certain metallic and clay bearing rocks. Measurements of IP were made in the time domain using the current waveform and signal format shown in figure 3. The primary voltage across the potential electrodes was recorded for resistivity determinations. The transient decay voltage integrated over the time interval shown in figure 3 was normalized by the primary voltage such that the induced polarization effect was read as a dimensionless quantity or the ratio of the secondary voltage to the primary voltage.

Compressional sonic velocity measurements were made on the natural state core samples using a pulse technique similar to that described by Obert and Duvall (1967). The sample was mounted between two bearing plates which allowed for axial loading at moderate pressures. Piezoelectric transducers made of

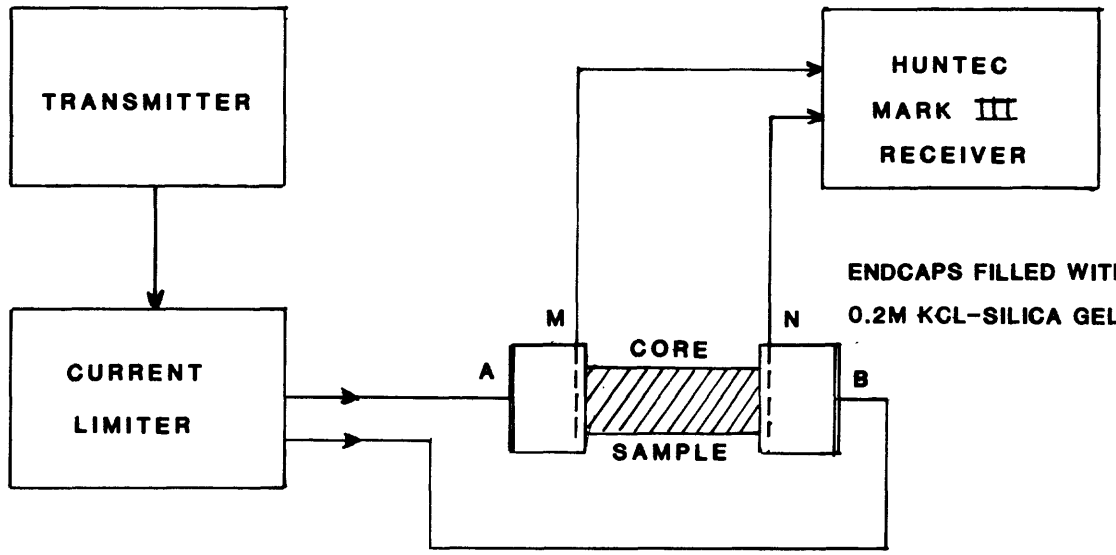

Figure 2- Block diagram of instrumentation used for d.c. resistivity and induced polarization measurements. The A and B and M and N symbols near the sample holder refer to the current and potential electrodes, respectively.

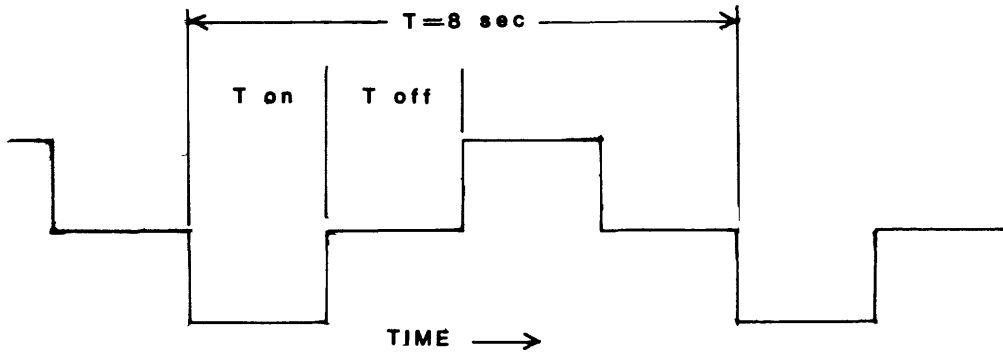

CURRENT WAVEFORM OUTPUT OF TRANSMITTER

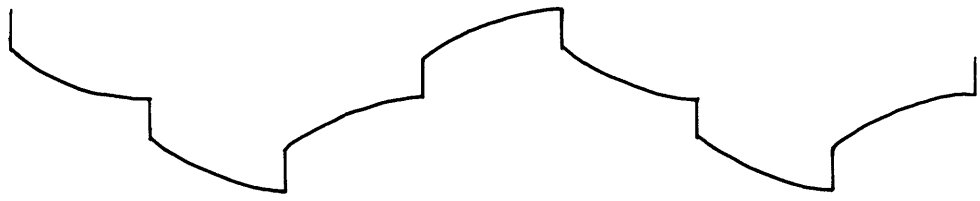

SIGNAL WAVEFORM AT INPUT TO RECEIVER

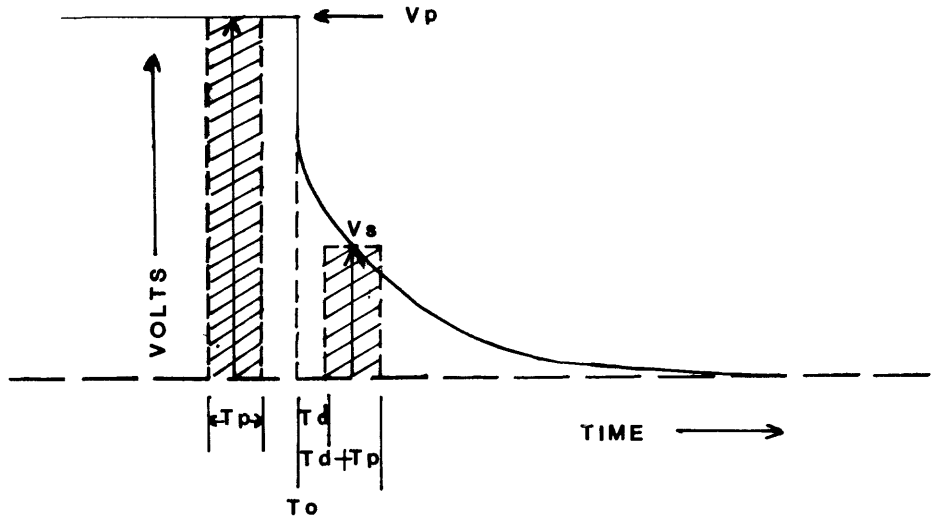

EXPANDED VIEW OF RECEIVED SIGNAL SHOWING INTERVALS OF PRIMARY AND SECONDARY VOLTAGE MEASUREMENT

Figure 3- Input and output signal waveforms at the current and potential electrodes of the sample holder used in the dc resistivity-induced polarization measurement. The lowermost waveform indicates the signal sampling intervals for the primary voltage (Vp) and the transient voltage (Vs). Tp is the integrating time for both Vp and Vs which in this instance was 30 milliseconds. The time delay (Td) following termination of current flow and transient voltage measurement was 15 milliseconds.

barium titanate crystals were mounted within each bearing plate in mechanical contact with the sample for energy transmission and detection. A high voltage pulse of less than 10 μs duration is converted to a compressional sonic wave through the crystal and is propagated through the sample, detected, recoverted to a voltage pulse, and displayed on an oscilloscope. Travel time of the transmitted signal through the sample is obtained by means of a delayed-sweep feature on the oscilloscope which provides for a direct reading of the time interval between the transmitted and received pulses. Propagation velocity of the compression wave, Vp, is calculated from the formula

$$Vp = L/(Tp-To); \qquad (2)$$

where L is the sample length; Tp, the apparent pulse travel time through the sample; and To, the zero time factor caused by time delay at the sample and transducer interfaces. The zero time factor was determined by measuring the system travel time using four 40 mm diameter aluminum rod varying in length from 50 to 90 mm. The resulting travel times were plotted as a function of rod length and the line connecting the data points extrapolated to the zero length intercept to determine the zero time correction value.

Prior to measurement the end surfaces of the core were lapped parallel to within 0.1 mm and the opposing faces coated with a thin layer of high-vacuum grease to assure good coupling between sample and transducers. Upon completion of the acoustic velocity measurements the grease coating the end surfaces of the core samples was removed with acetone and again lapped to remove the last traces of any remaining grease.

Following the foregoing measurements made on natural-state cores, the samples were prepared for density and porosity determinations. Procedures used in this phase of the laboratory activity are described by Johnson (1979). Samples were dried, weighed and then saturated with tap water and subsequently weighed both in

air and suspended in water. Rock volume was obtained using a water displacement technique discussed in Chleborad and others (1975). From these data dry bulk density, DBD, saturated bulk-density, SBD, grain density, GD, and fractional porosity, ϕ, were computed as follows:

$$DBD = \frac{Wd}{V} ; \qquad (3)$$

$$SBD = \frac{Ws}{V} ; \qquad (4)$$

$$\phi = \frac{Ws-Wd}{V} ; \qquad (5)$$

$$GD = \frac{DBD}{1-\phi} , \qquad (6)$$

where Wd and Ws are dry and saturated sample weights, respectively, and V is the bulk volume of the rock.

Natural remanent magnetization (NRM) was determined from measurements made with a Schonstedt SSM-1A spinner magnetometer using a three-spin technique as described by Watson (1979). Prior to measurement, each sample was reduced in size to a cylinder 25.4 mm (1 in) in both diameter and length to conform to the sample size specifications set forth for use with the Schonstedt instrument. Individual measurements of magnetic moment of x, y, and z (rectangular coordinate system) in cgs units are resolved in terms of remanent magnetic intensity and remanent vector orientation but, because the in-place azimuths of the Yucca Mountain cores are unknown, only the inclination of the vector is meaningful.

Magnetic susceptibility was measured with the direct-reading model 3101 Bison susceptibility meter and converted to induced magnetization by multiplying the measured magnetic susceptibility value by 41.38 amp/m, the earth's total magnetic field intensity at NTS in SI units.

Koenigsberger's Q ratio, the numerical quotient of the remanent magnetization divided by induced magnetization, was determined as an indicator of the relative intensities of the two components of magnetization.

Water permeabilities were measured on 25.4 mm (1 in) water saturated core as shown in figure 4. The enclosing or confining pressure was nominally maintained at 100 psi while fluid under a driving pressure of 50 psi was forced through the sample along the line of its principal axis. Water flow was allowed to reach equilibrium before a series of readings were made to determine the nature of permeability changes with time. The rate of flow of a fixed volume of water through a 1.6 mm diameter capillary was timed and permeability (K_D) calculated from the equation

$$K_D = \frac{\mu V l}{T \Delta P A} \qquad (7)$$

where V is volume of water, T is time, μ is water viscosity at 20°C, A and l the cross-sectional area and length of the sample respectively, ΔP, the net pressure difference across the length of the sample in atmospheres. The hydraulic unit used herein is call a Darcy.

Laboratory Results

Resistivity, bulk-density, and compressional sonic velocity measurements were first made on samples as they were uncovered from their beeswax casing. The interest in obtaining as much information as possible in the initial stages of laboratory measurement is twofold in as much as the in place character of the rock is best exemplified when in its natural state, and, according to Spengler and others (1979), much of the rock, particularly within the Tiva Canyon and Topopah Springs Members of the Paintbrush Tuff, is considered to be structurally incompetent; therefore subsequent core loss could be anticipated in the course of sample handling and preparation.

Electrical Measurements

The results of the total number of resistivity and induced polarization measurements made are listed in Table 1. Resistivities measured at 100 Hz for natural-state and resaturated samples are plotted in figure 5 with respect to

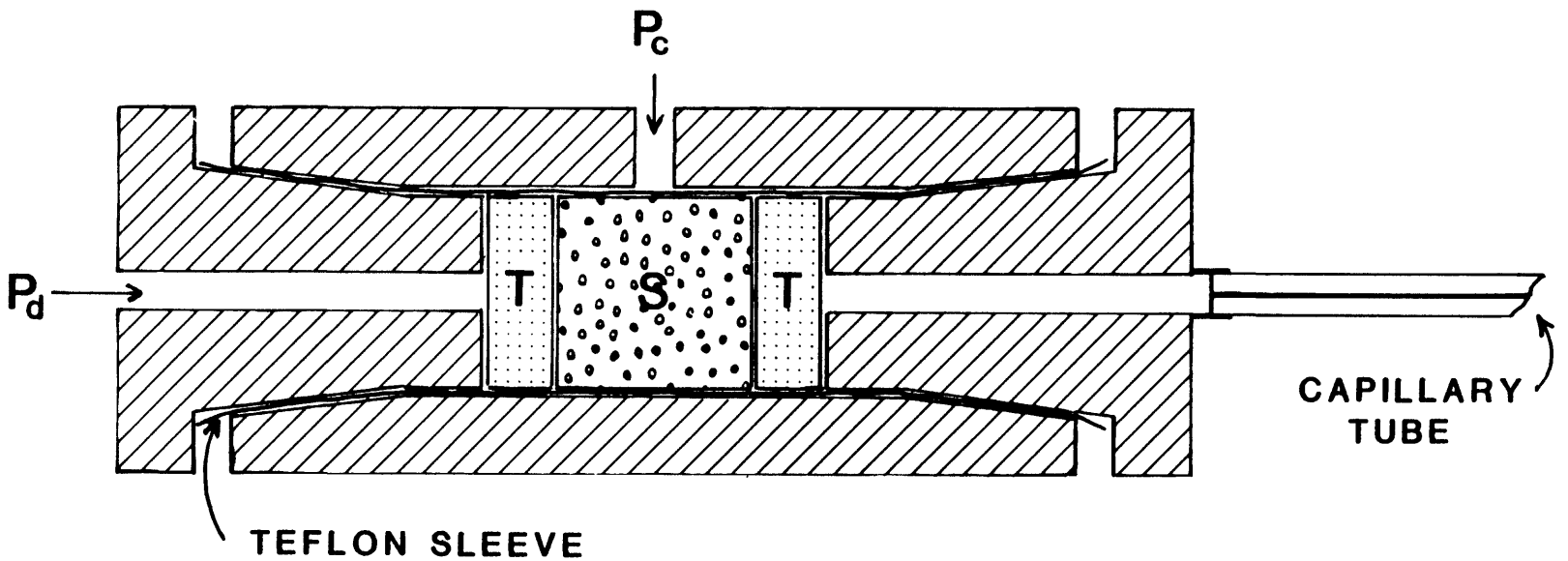

Figure 4- Diagram of the stainless steel hydraulic conductivity cell used for permeability measurements. Porous teflon spacers, T, are designed to direct water flow uniformly through the sample, S, under confining pressure, Pc, and driving pressure, Pd, of 100 and 50 psi, respectively. The capillary tube is used to measure the rate of water flow through the rock.

TABLE I

Values of electrical resistivity and induced polarization for natural state and saturated samples.

[Leader (-) indicates no measurement possible]

Sample depth in feet (meters)	100 Hz resistivity in ohm-m		dc resistivity in ohm-m (saturated)	Induced polarization in percent
	natural state	saturated		
58 (17.7)	1930	2245	2473	1.7
102 (31.1)	1043	990	1110	1.3
153 (46.6)	1570	1574	1833	1.6
187 (57.0)	340	218	238	2.7
202 (61.6)	86	95	104	1.7
212 (64.6)	21	15	18	3.3
234 (71.3)	29	23	24	3.6
263 (80.2)	72	32	39	3.0
273 (83.2)	360	-	-	-
328 (100)	1446	630	635	1.6
360 (109.8)	1137	718	727	2.4
421 (128.4)	277	274	327	3.6
471 (143.6)	440	230	278	3.4
524 (159.8)	251	156	179	1.8
569 (173.5)	313	220	271	2.2
623 (189.9)	536	380	394	2.0
660 (201.2)	1510	1200	1310	1.0
733 (233.5)	765	654	767	1.9
772 (235.4)	924	633	703	2.2
816 (248.8)	990	1120	1210	2.0
866 (264.0)	1650	1343	1541	2.3
921 (280.8)	1970	1237	1428	1.9
969 (295.4)	1770	789	902	1.2
1010 (307.9)	1322	893	963	1.9
1040 (317.1)	752	623	656	1.6
1112 (339.0)	2260	1690	1990	2.1
1183 (360.7)	1965	1535	1770	2.2
1249 (380.8)	675	757	654	1.6

TABLE I (con't)

Sample depth in feet (meters)	100 Hz resistivity in ohm-m natural state	100 Hz resistivity in ohm-m saturated	dc resistivity in ohm-m (saturated)	Induced polarization in percent
1266 (386.0)	500	353	366	1.8
1305 (397.9)	2545	2990	3045	1.0
1324 (403.7)	107	80	76	1.0
1338 (407.9)	405	458	344	1.2
1349 (411.3)	141	122	124	1.4
1361 (414.9)	178	119	112	1.8
1411 (430.2)	224	132	133	1.3
1464 (446.3)	121	88	95	1.5
1516 (462.2)	85	61	60	1.9
1568 (478.0)	80	57	61	1.4
1638 (499.4)	110	69	64	1.7
1687 (514.3)	134	93	86	0.8
1740 (530.5)	84	58	55	1.3
1792 (546.3)	36	32	32	0.5
1833 (558.8)	38	35	36	0.4
1842 (561.6)	124	60	66	1.5
1888 (575.6)	104	77	72	2.9
1942 (592.1)	94	78	82	1.6
1987 (605.8)	1078	715	795	1.4
2031 (619.2)	152	105	103	2.1
2078 (633.5)	408	287	297	2.9
2108 (642.7)	331	243	244	0.9
2149 (655.2)	102	93	101	1.7
2159 (658.2)	10490	2776	2892	2.4
2201 (671.0)	577	498	502	0.8
2247 (685.1)	267	205	190	1.1
2301 (701.5)	323	295	302	1.8
2330 (710.4)	231	198	201	1.0
2377 (724.7)	235	110	127	2.0
2440 (743.9)	191	138	135	2.2
2495 (760.7)	148	97	107	4.5

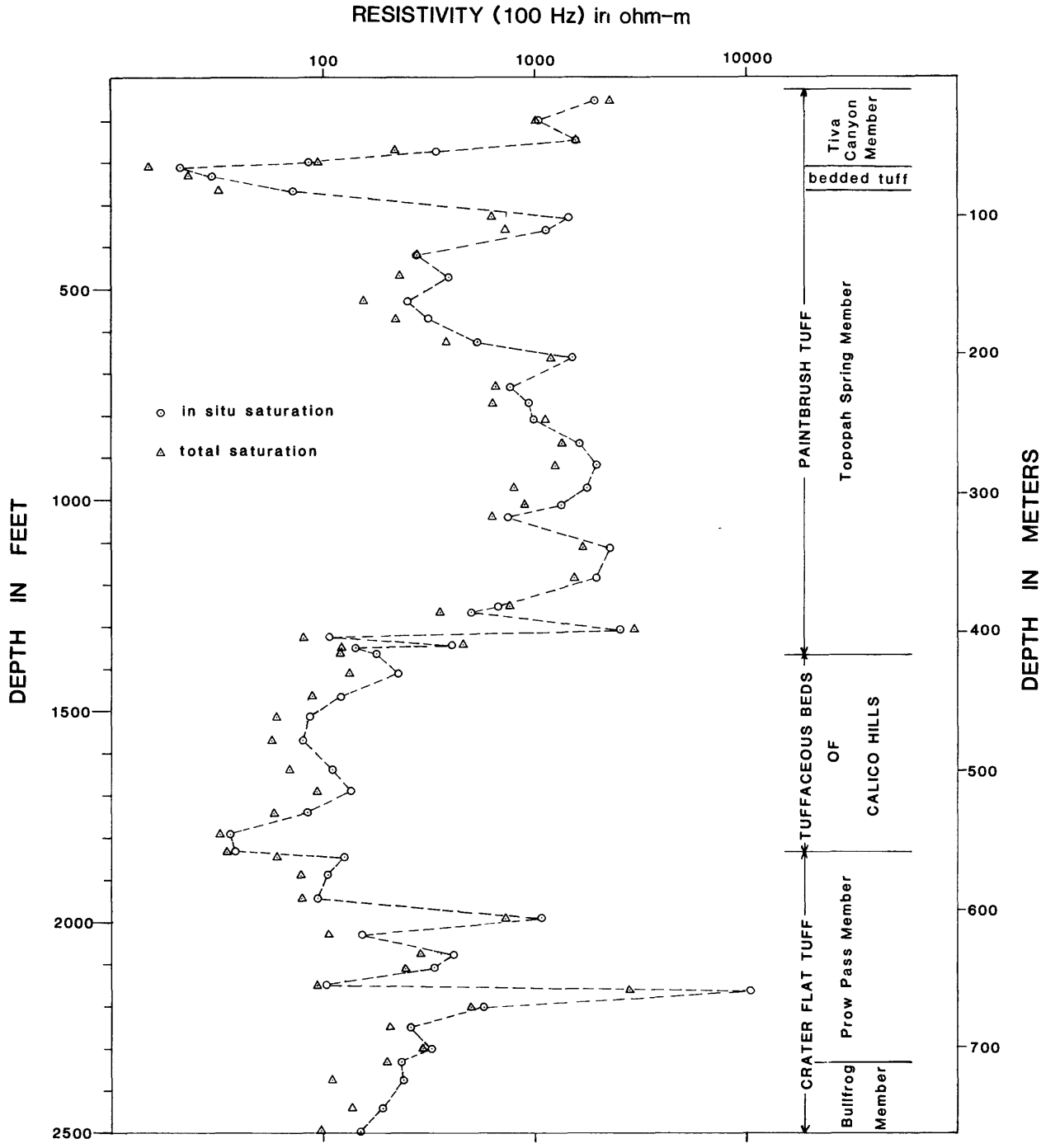

Figure 5- Resistivity values of natural-state and resaturated core samples plotted against depth of origin. Dashed line connects the natural state data points to demonstrate resistivity variations with depth.

their depth of origin. With few exceptions the resistivities of the natural state sample are somewhat higher than the resistivities of the resaturated samples as the result of a lower water content, an observation which also holds true for those samples taken from below the static water level at 470 m (1542 feet) and are expected to be fully water saturated. Evidently some degree of dehydration had occurred between the time of core extraction from the borehole and the time of encasement in beeswax. Samples having equal or greater resistivities when resaturated than when in the natural state mode are all of low porosity suggesting that incomplete resaturation produced a higher than normal resistivity. The discrepancy may also relate to differences in resistivity of the water within the natural and resaturated core.

With few exceptions resistivity differences between corresponding data points do not alter the character of the resistivity variations observed in both natural state and resaturated sample measurements. Although compositional and textural differences occur within the units of tuff intersected by the borehole, resistivities are largely controlled by porosity. This dependence can be seen by comparing the resistivity plot (figure 5) with the porosity plot shown in figure 6. The inverse relationship between resistivity and porosity is virtually preserved throughout the entire measured section.

In the uppermost Tiva Canyon Member of the Paintbrush Tuff the near surface ash-flow tuffs are densely welded and well compacted and, as such, produce resistivities in excess of 1000 ohm-m. In the interval, 53-83 meters (173-270 feet), the tuff is non-welded to moderately welded and, accordingly, its resistivity is as low as 15 ohm-m with a corresponding porosity of almost 53 percent. The rock within this interval has been somewhat argillized therefore the relationship between porosity and resistivity is not exact because of the conductive properties of the clay minerals within the argillite itself.

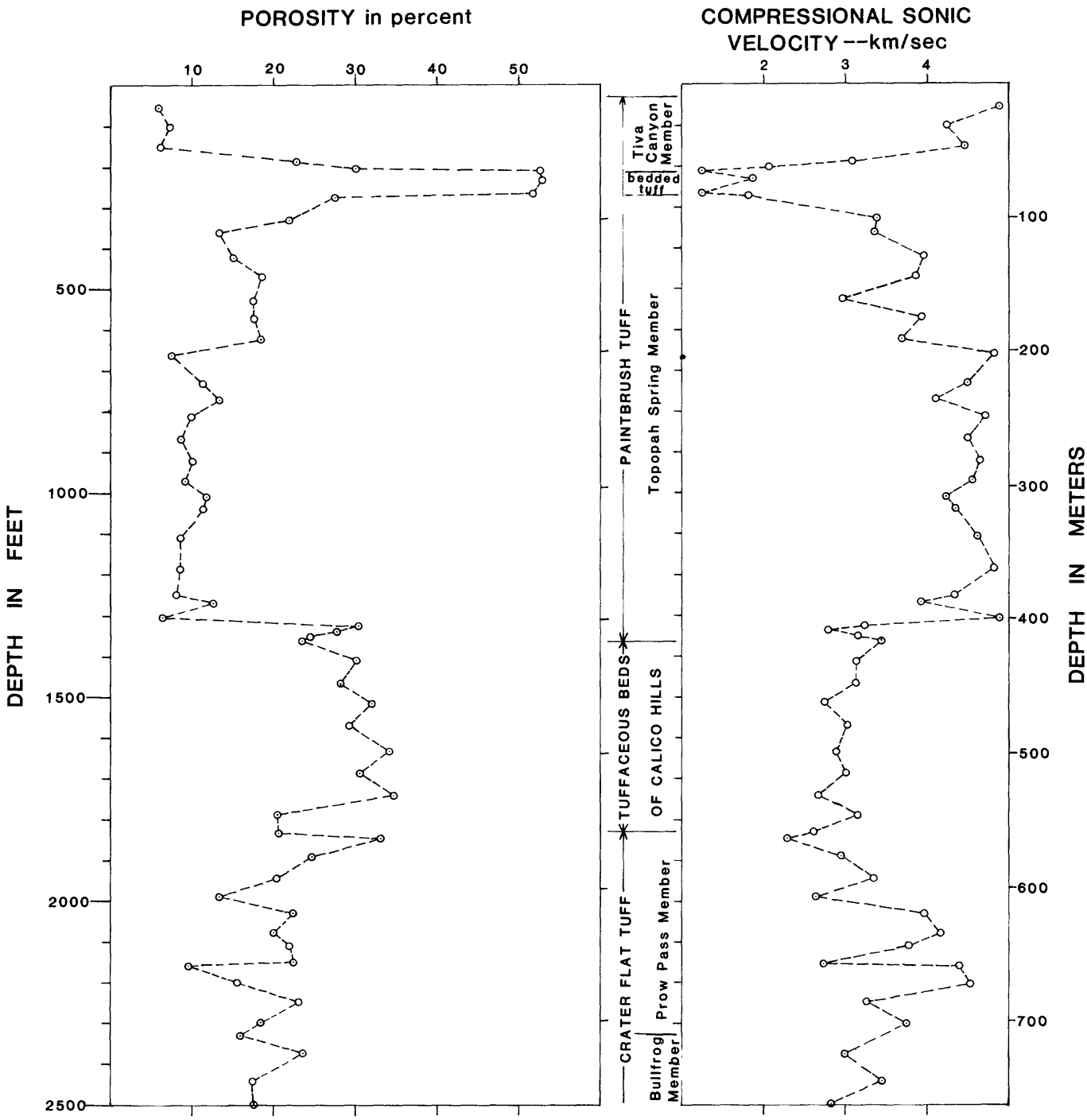

Figure 6- Porosity and compressional sonic velocity values for borehole samples plotted as a function of depth of origin. Dashed lines indicate rock property variations with depth.

The resistivity of the Topopah Spring Member is generally high; particularly within the lower 2/3 of the unit showing an inverse correlation with porosity. Although the extent to which the tuffs are welded has some effect on the resistivity, the latter is most influenced by the existence of spherical cavities within specific intervals of the tuff. The thickest of these lithophysal zones (Spengler and others, 1979) is located approximately in the 122 to 191 meter interval (400-625 feet) and is characterized by a relatively low resistivity. Secondary minerals partially fill the cavities; nevertheless, the total porosity is still sufficiently increased to cause a significant decrease in resistivity. At the 396 meter lever (1300 feet) the resistivity changes rapidly as the rock varies from a densely welded vitrophyre to a non-welded devitrified variety of tuff near the 403 meter (1322 feet) depth. At the base of the Topopah Spring Member the resistivites of the tuffs are very similar to those of the underlying beds of Calico Hills such that the contact, as identified by Spengler and others (1979), is virtually impossible to recognize on the basis of electrical measurements. The resistivities of the tuff beds of Calico Hills are appreciably lower than the tuffs forming the bulk of the Topopah Springs unit primarily as the result of a correspondingly higher porosity. The samples obtained from the beds of Calico Hills are basically volcanic breccias containing large inclusions of pumice which may explain the high porosity-low resistivity relationship. Resistivities of those samples taken from the lower 13.7 meter (45 feet) base interval are the lowest found for consolidated tuffs penetrated in the borehole and, paradoxically, are associated with an approximate 33 percent decrease in water accessible porosity from the average porosity determined for the tuffs of Calico Hills. The phenocrysts within the samples from the base interval are smaller and somewhat more numerous than those which are visible in the samples from the upper interval of the Calico Hills. It is not readily

apparent what is causing the decrease in resistivity. Clay alteration is a possible cause but its likelihood is not supported by the induced polarization response. The wider distribution of the pumice within the samples of the base interval may enhance the distribution of current flow through the rock thereby lowering the bulk resistivity of the rock.

The resistivities of samples from the Prow Pass Member of the Crater Flat Tuff are highly variable as a function of changes in texture, the degree to which the tuffs have been welded, and the intensity of silicification. At the extreme top of the Prow Pass Member the tuff is nonwelded and similar in resistivity to the upper section of the Calico Hills. In the central section the rocks are moderately welded and show a general increase in resistivity with peak resistivities occurring at the 606 m (1988 feet) and 658 m (2159 feet) depths where the rocks are well silicified. The lowermost tuffs of the Prow Pass Member decline in resistivity with depth as they grade into the Bullfrog Member indicating a general decrease in the level of welding which occurs within this interval of the Crater Flat Tuff. Comparing resistivity and porosity plots covering the Crater Flat section it is evident that porosity variations are principally responsible for the resistivity changes observed within the interval.

Resistivity and IP data obtained on resaturated samples using the Huntec receiver at near dc frequency are listed in Table I and are shown plotted against depth in figure 7. For the most part the dc resistivities are slightly higher than those measured at 100 Hz because of the frequency dependence of the dielectric constant of the rock but the difference is inconsequential and the character of the original resistivity plot is maintained.

The IP values are quite low throughout the entire section averaging about 2 percent, which is considered to be a normal background level (Mayper, 1959). Within the Paintbrush Tuff the anomalous polarization zones peak at the 72 meter (235 feet) and 128 meter (420 feet) depths. The 72 meter anomaly can be

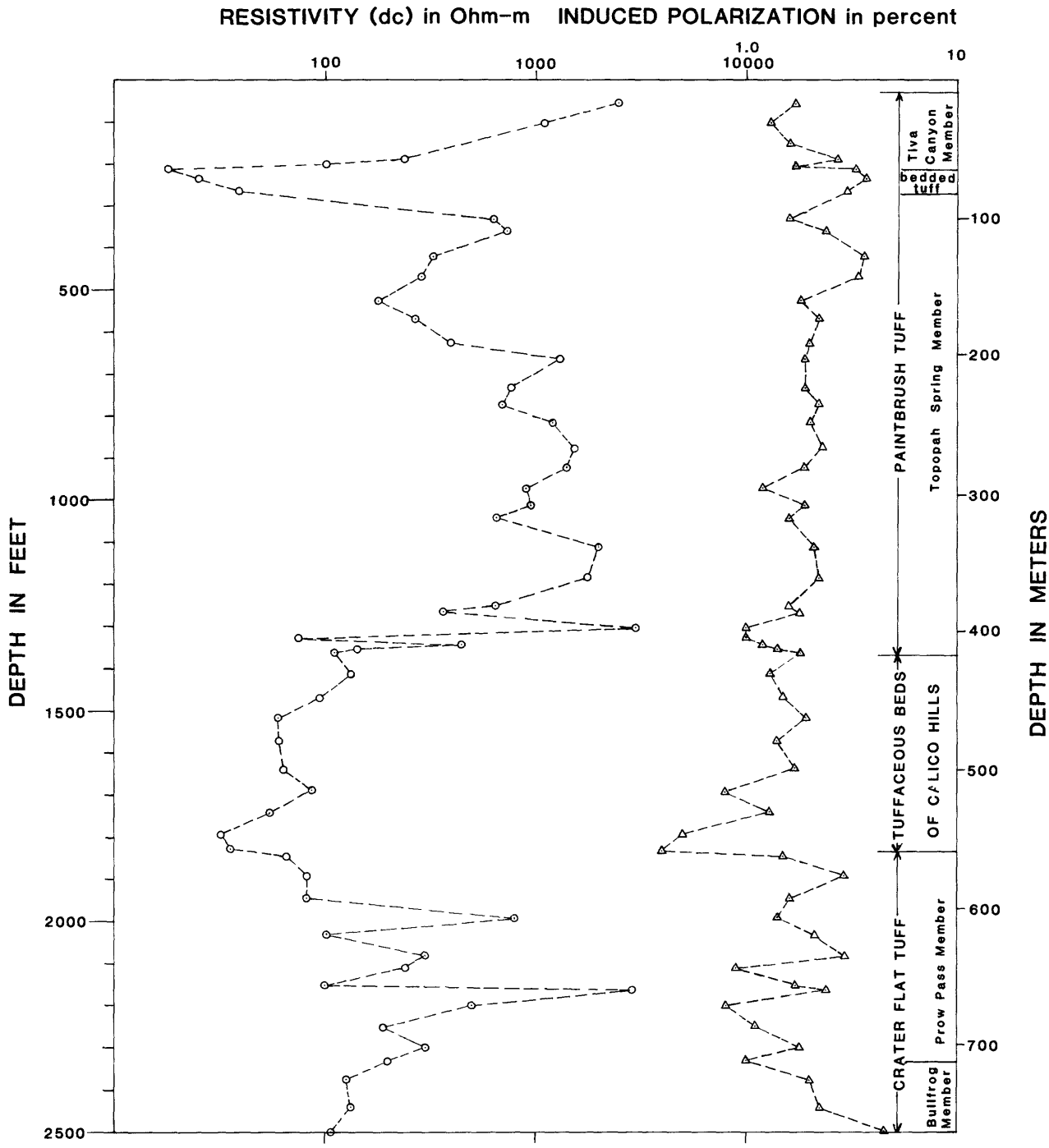

Figure 7- DC resistivity and induced polarization values of individual borehole samples plotted as a function of depth of origin. Resistivity is shown on the left and each data set is connected by dashed lines to indicate variations with depth.

attributed to clay polarization (Sumner, 1976) produced by the argillite in the poorly consolidated bedded tuffs at the base of the Tiva Canyon Member. The cause of the 128 meter anomaly near the top of the Topopah Spring unit can not be readily identified from the physical appearance of the rock but the fact that the anomaly is of the same amplitude as is the anomaly at the 72 meter depth suggests the probability of clay as the source of the polarization. Magnetite can be found within the Paintbrush Tuff in minute quantities but its presence is obviously not sufficient to generate a polarization response.

The I.P. effect continues to diminish with depth until the lowest values encountered within the sample group are found among those taken from near the base of the tuffaceous beds of Calico Hills. A marked increase in polarization occurs at the Crater Flat Tuff contact, rising to the normal background level but showing high variability with depth as a function of the texture and mineral composition of the rock. The highest polarization values were measured on samples from the Bullfrog Member of the Crater Flat Tuff for which there is no obvious explanation although the I.P. effect is probably caused by clays and possibly zeolites within a partial to moderately welded matrix.

Density Measurements

Measured values of natural bulk density, (NBD); saturated bulk density, (SBD); dry bulk density, (DBD); and grain density, (GD) are listed in Table II and, with the exception of grain density, are plotted against depth of origin in figure 8. Sample porosity, ϕ, calculated from density and volume determinations, are listed in Table III along with sonic compressional velocity and hydraulic conductivity data. Density variations within the penetrated section are indicated by the dashed line drawn through the NBD data points in figure 8. The plot can probably be viewed as a definitive portrayal of the manner with which textural changes occur between and within the intersected stratigraphic units.

TABLE II

Values of natural bulk density (NBD), saturated bulk density (SBD), dry bulk density (DBD), and grain density (GD).

Samples depth in feet (meters)	NBD Mg/m^3	SBD Mg/m^3	DBD Mg/m^3	GD Mg/m^3
58 (17.7)	2.35	2.39	2.33	2.48
102 (31.1)	2.36	2.38	2.31	2.49
153 (46.7)	2.36	2.39	2.33	2.48
187 (57.0)	2.07	2.10	1.87	2.43
202 (61.6)	1.97	2.0	1.69	2.43
212 (64.6)	1.56	1.66	1.14	2.41
234 (71.3)	1.50	1.67	1.14	2.43
263 (80.2)	1.45	1.68	1.16	2.41
273 (83.2)	1.75	1.86	1.58	2.18
328 (100.0)	2.12	2.23	2.01	2.57
360 (109.8)	2.26	2.34	2.21	2.55
421 (128.4)	2.12	2.28	2.13	2.51
471 (143.6)	1.93	2.21	2.02	2.49
524 (159.8)	2.1	2.21	2.04	2.47
569 (173.5)	2.12	2.27	2.09	2.54
623 (189.9)	2.21	2.28	2.10	2.57
660 (201.2)	2.38	2.39	2.32	2.51
733 (223.5)	2.35	2.36	2.25	2.54
772 (235.4)	2.32	2.36	2.23	2.57
816 (248.8)	2.39	2.41	2.31	2.56
866 (264.0)	2.42	2.44	2.35	2.57
921 (280.8)	2.34	2.41	2.31	2.54
969 (295.4)	2.38	2.40	2.31	2.54
1010 (307.9)	2.33	2.34	2.23	2.52
1040 (317.1)	2.33	2.36	2.25	2.53
1112 (339.0)	2.36	2.4	2.31	2.53
1183 (360.7)	2.42	2.44	2.36	2.57
1249 (380.8)	2.39	2.41	2.33	2.54
1266 (386.0)	2.25	2.29	2.16	2.48
1304 (397.6)	2.23	2.28	2.21	2.36

TABLE II (con't)

Samples depth in feet (meters)	NBD Mg/m^3	SBD Mg/m^3	DBD Mg/m^3	GD Mg/m^3
1324 (403.7)	1.89	1.93	1.62	2.33
1338 (407.9)	1.77	1.80	1.53	2.11
1349 (411.3)	2.0	2.0	1.76	2.32
1361 (414.9)	1.99	2.0	1.77	2.31
1411 (430.2)	1.92	1.93	1.63	2.33
1464 (446.3)	1.95	1.97	1.69	2.35
1516 (462.2)	1.89	1.91	1.59	2.35
1568 (478.1)	1.93	1.97	1.68	2.37
1638 (499.4)	1.81	1.87	1.53	2.33
1686 (514.0)	1.89	1.92	1.62	2.33
1741 (530.8)	1.87	1.90	1.56	2.36
1791 (546.0)	2.19	2.20	1.99	2.50
1833 (558.8)	2.13	2.13	1.93	2.43
1842 (561.6)	1.89	1.91	1.58	2.37
1888 (575.6)	2.17	2.20	1.96	2.60
1942 (592.1)	2.24	2.28	2.07	2.60
1988 (606.1)	2.35	2.39	2.26	2.60
2032 (619.5)	2.15	2.20	1.97	2.54
2078 (633.5)	2.21	2.21	2.01	2.50
2108 (642.7)	2.04	2.08	1.86	2.39
2149 (655.2)	1.96	1.95	1.72	2.22
2159 (658.2)	2.23	2.24	2.14	2.37
2201 (671.0)	2.13	2.14	1.98	2.34
2247 (685.1)	2.03	2.04	1.81	2.35
2300 (701.2)	2.14	2.15	1.97	2.41
2331 (710.7)	2.18	2.19	2.03	2.42
2377 (724.7)	2.20	2.23	1.99	2.61
2440 (743.9)	2.29	2.31	2.14	2.59
2495 (760.7)	2.29	2.32	2.14	2.59

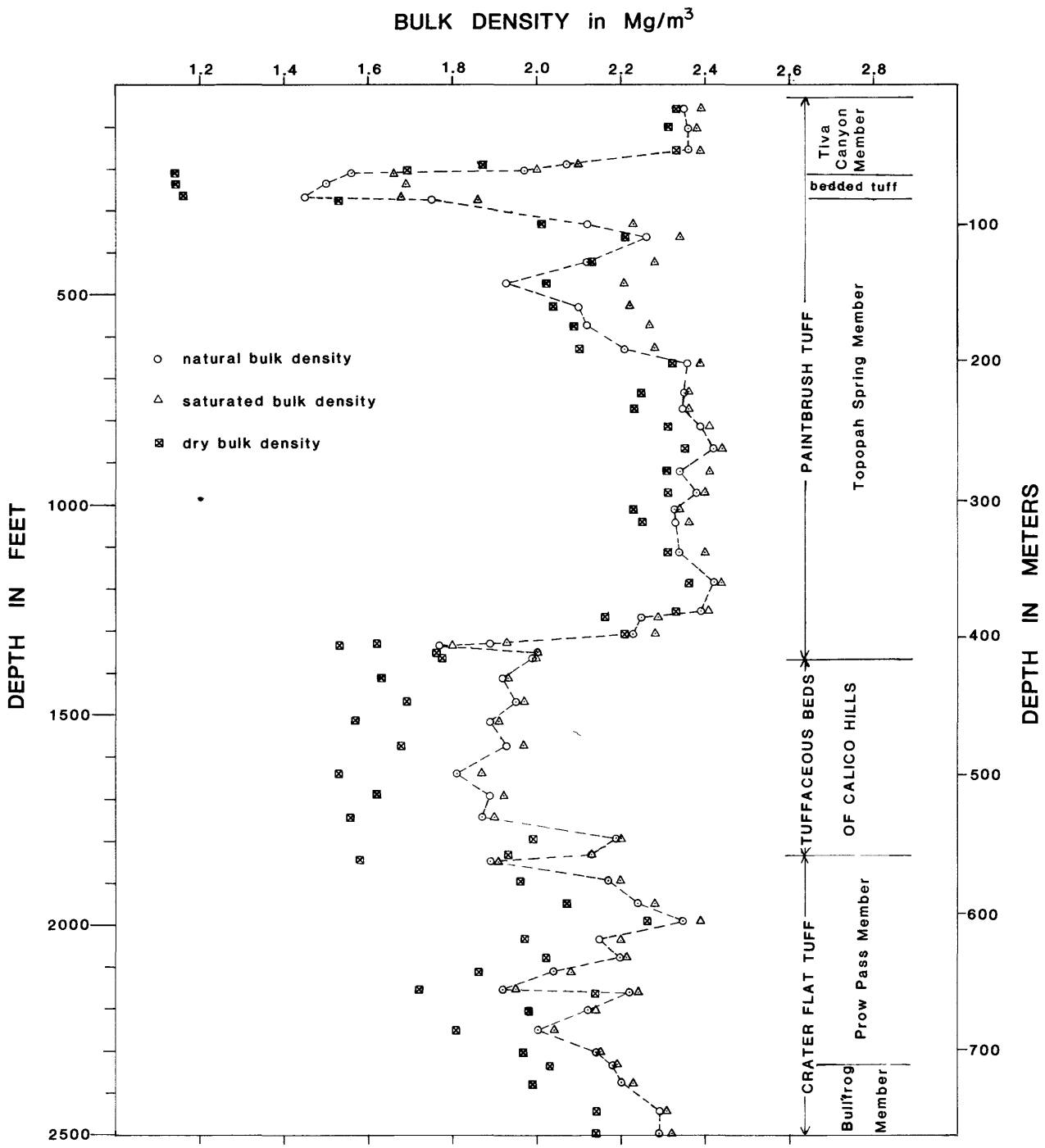

Figure 8- Bulk density values for core samples plotted as a function of depth of origin. The dashed line connects natural bulk density values to aid in demonstrating variations with depth.

TABLE III

Values of porosity, compressional sonic velocity,

and hydraulic conductivity

[Leader (-) indicates no measurement possible]

Sample depth in feet (meters)	Porosity in percent	Compressional sonic velocity in Km/sec	Hydraulic conductivity in μDarcies
58 (17.7)	6.0	4.89	0.186
102 (31.1)	7.3	4.24	2.90
153 (46.7)	6.14	4.46	3.55-2.49
			reversed flow 3.45-2.58
187 (57.0)	22.9	3.09	50.0
202 (61.6)	30.1	2.76	1.39
212 (64.6)	52.7	1.25	-
234 (71.3)	52.9	1.88	-
263 (80.2)	51.7	1.27	-
273 (83.2)	27.4	1.81	-
328 (100.0)	21.9	3.39	52.7-25.3
360 (109.8)	13.3	3.35	-
421 (128.4)	15.0	3.96	1.91-1.57
471 (143.6)	18.6	3.87	14.7-11.0
524 (159.8)	17.6	2.97	610-489
569 (173.5)	17.7	3.93	-
623 (189.9)	18.4	3.69	-
660 (201.2)	7.5	4.81	5.5-3.6
733 (223.5)	11.3	4.5	3.42-1.23
772 (235.4)	13.3	4.11	188.5-51.4
816 (248.8)	9.8	4.70	0.80
866 (264.0)	8.65	4.50	1.67
921 (280.8)	10.0	4.64	1.15
1010 (307.9)	11.8	4.24	1.32
1040 (317.1)	11.2	4.35	14.2-13.5
1112 (339.0)	8.7	4.62	3.82-2.48
1183 (360.7)	8.5	4.82	12.5-3.3
1249 (380.8)	8.03	4.34	2.9
1266 (386.0)	12.7	3.92	161-26.2

TABLE III (con't)

Sample depth in feet (meters)	Porosity in percent	Compressional sonic velocity in Km/sec	Hydraulic conductivity in μDarcies
1304 (397.6)	6.28	4.89	8.1-3.58
1324 (403.7)	30.3	3.24	-
1338 (407.9)	27.7	2.80	-
1349 (411.3)	24.4	3.15	-
1361 (414.9)	23.4	3.43	51.9-40.6
1411 (430.2)	30.1	3.13	-
1464 (446.3)	28.1	3.13	-
1516 (462.2)	32.1	2.74	17.2-12.5
1568 (478.1)	29.3	3.03	241
1638 (499.4)	34.1	1.89	366
1686 (514.0)	30.7	3.02	-
1741 (530.8)	33.8	2.68	52.2
1791 (546.0)	20.4	3.15	4.52
1833 (558.8)	20.7	2.61	-
1842 (561.6)	33.1	2.3	61.3
1888 (575.6)	24.7	2.95	1694-1537
1942 (592.1)	20.3	3.31	78-72
1988 (606.1)	13.3	2.63	183-114
2032 (619.5)	22.3	3.97	60.7-28.5
2078 (633.5)	20.0	4.16	137-50
2108 (642.7)	21.9	3.78	311-240
2148 (655.2)	22.3	2.74	-
2159 (658.2)	9.68	4.39	121-113
2201 (671.0)	15.4	4.53	1043-1034
2247 (885.1)	23.0	3.27	-
2300 (701.2)	18.4	3.75	-
2331 (710.7)	15.9	4.14	-
2377 (724.7)	23.5	3.0	1571-1521
2440 (743.9)	17.5	3.44	228-219
2495 (760.7)	17.4	2.82	499-473

Obvious differences in density within individual samples exist as a function of water content when comparing the three data sets. Density extremes are most evident amongst those samples having the higher porosities. With few exceptions the NBD values fall somewhere between those obtained for dry and resaturated sample measurements. Differences between the NBD and SBD data are generally small amounting to only a few percent and may be the result of dehydration having occurred between the time of extraction from the borehole and the time at which the core was sealed in beeswax. That dehydration has taken place seems evident from the fact that the rock below the static water level (approximately 470 meters (1542 feet) at the time of drilling), which is expected to be totally saturated, has NBD values below those of SBD. However, the small observed offsets between data sets in the section below the water table may be artificial because of errors inherent in a calipered volume determination as opposed to the more accurate water-displacement technique used in arriving at the SBD, DBD, and GD values for well-compacted rock. An obvious example of volume error exists in the 137 to 152-meter interval (450-500 feet) where DBD values exceed those of NBD. In this upper interval of the Topopah Spring Member, lithophysal cavities are abundant in the densely welded tuff (Spengler and others, 1979) therefore the apparent bulk rock volume determined by the water displacement method is well below that which actually exists.

Not all NBD-SBD differences can be totally attributed to measurement error. In the high porosity bedded tuffs at the base of the Tiva Canyon Member it is suspected that some degree of water loss has occurred through dehydration. Despite the apparent measurement errors encountered in sample handling the stratigraphic recognition pattern is preserved in each suite of density determinations although it is believed that the SBD values most nearly approximate those of the in place rock.

The GD values listed in Table II show variations which are attributed to compositional differences brought about by alteration processes. The formation of clays and zeolites within the tuffs of Calico Hills occupying the 416-560 meter interval (1364-1836 feet) has caused a decrease in grain density of virtually the entire unit whereas only the lower part of the Prow Pass Member of the Crater Flat Tuff in the 610-723 meter interval (2000-2370 feet) has been altered. Other stratigraphic units have been similarly affected but to a lesser extent. The bedded tuff at the base of the Tiva Canyon Member in the 217-270 m interval (66.1-82.3 feet) is composed largely of pumice which generally has a low apparent grain density because of voids sealed within its grain structure. As an example, pumice from Mount St. Helens has an apparent grain density of less than 2.0 Mg/m^3 as determined by the water displacement method (Olhoeft and others, 1981), but its intrinsic grain density, measured on finely powdered material, is 2.60 Mg/m^3 (G. R. Johnson, oral communication, 1981).

Compressional Sonic Velocity

Compressional sonic velocities measured at near in situ water saturation levels are shown in figure 6 plotted along with porosity as a function of depth of origin. The effect of porosity on sonic velocity is clearly evident from the inverse relationship existing between these two rock properties. The highest velocities occur within the densely welded tuffs of the Paintbrush Tuff although acoustic attenuation is apparent near the top of the Topopah Spring Member where cavities within the welded tuff constitute as much as 30 percent of the bulk volume of rock thereby forming an impediment along the acoustic propagation path and hence, attenuation of the seismic signal. Sonic velocities as low as 1.25 km/sec were measured for the poorly consolidated bedded tuffs at the base of the Tiva Canyon Member.

The acoustic velocities of the tuff of Calico Hills average about 4.0 km/s

but indicate a slight velocity decrease with depth with the greatest variability taking place near the base of the formation. These fluctuations persist throughout the entire measured section of Crater Flat Tuff and, within well defined intervals where the ash-flow tuffs have been highly silicified, velocities approach those of the densely welded tuffs of the Paintbrush Tuff.

Hydraulic Conductivity

Hydraulic conductivity, better known as permeability, is a measure of how well the texture of a rock permits the passage of water under a fixed hydraulic gradient. The relative permeability values obtained are listed in Table III and have not been plotted in graphic form because of the high variability encountered within the individual stratigraphic units having similar porosities. Where only one value is indicated, the samples were either of very low permeability (<3.0 μDarcies) or produced no significant changes following the initial measurement. Many samples, however, show a decrease in permeability with time and the first and last values determined for a set of repeated measurements have been listed in Table III. The last value does not necessarily represent the lowest permeability attainable within a particular rock but rather a value which changed only slightly from the previous measurement.

Sample 153 was measured first with fluid flow in one direction and then reversed within the sample holder to obtain a measurement of water flow in the opposite direction. In both modes the beginning and ending values were essentially the same; the discrepancy caused by time differences between individual readings. The decrease in permeability with time is evidently caused by the redistribution of clay-sized particles so as to effectively close off some of the capillaries connecting the pore spaces of the rock. The apparent internal mobility of the constituent particulate matter within the pore spaces adds another controlling element to rock permeability which, according to Pirson

(1963), is normally dependent upon porosity, tortuosity, and grain size.

The gaps in the data set result from sample losses incurred during the reshaping process which primarily affected the poorly welded samples. Other samples proved unsuitable for measurement because of the size of the contained lithophysal cavities. However, from those sample permeabilities measured, the indications are that the densely welded tuffs of the Paintbrush Tuff rarely exceed tens of microdarcies as their final value. An exception is the sample from the 159.8 m level (524 feet) whose terminal permeability values is 489 μ-Darcies. This is a rather poor sample because of its secondary mineral content which forms a somewhat pockmarked core surface and, more seriously, an incomplete crack in the axial direction of the core provided a preferential path for water migration thereby dramatically increasing its apparent permeability. According to Spengler and others, 1979, the Paintbrush Tuff is highly fractured as are parts of the Prow Pass Member of the Crater Flat Tuff; therefore fracture porosity conceivably plays a more important role than intergranular porosity in controlling permeability within these stratigraphic units and perhaps within the entire penetrated section. As measured, the listed values represent the lower limits of permeability with the upper limit as characterized by in-place rock conditions not possible to define through sample analysis.

The formation underlying the Paintbrush Tuff show a general increase in permeability with depth although a high degree of variability is evident within each member. Samples from this lower interval are unfractured therefore the permeability changes occur as the result of differences in the textural properties of the rock.

Magnetic Properties

Magnetic susceptibility, remanent magnetization, induced magnetization, remanent vector inclination, and Koenigsberger ratios for those samples available

for measurement have been listed in Table IV. The magnetic susceptibility and magnetization components were converted from cgs and mks units to conform to the International System of Units (SI). Remanent and induced magnetic values plotted in figure 9 graphically demonstrate the greater intensity of remanence for virtually all samples measured and the dramatic decrease in rock magnetization at the contact of the Paintbrush Tuff and the tuffs of Calico Hills. As seen in Table IV the Tiva Canyon Member of the Paintbrush tuff has a remanent component of magnetization whose direction is reversed with respect to the present day normal field alignment. Variations in magnetic susceptibility and hence the induced component of magnetization are greatest in the upper half of the Topopah Spring Member as a reflection of differences in the magnetic mineral content.

Beneath the Topopah Spring Member the magnetic properties of the rock are so variable that recognition of formation contacts on the basis of magnetics becomes virtually impossible. The rapid changes in the induced magnetic field demonstrate the effects of differences in magnetite content within individual ash-flow subunits.

The Koenigsberger ratio, Q, which is the remanent magnetic intensity divided by the product of magnetic susceptibility and the inducing field, is an estimate of the relative importance of the remanent magnetization as compared to the induced magnetization as a contributing element in the generation of magnetic anomalies. With only one exception the Koenigsberger ratios for the core samples exceed the value of 1.0, indicative of the strength of the remanent magnetization as compared to that of the induced component. Exclusive of the Tiva Canyon Member the magnetic patterns produced by the various stratigraphic units should normally not cause undue concern because the inclination of the remanent vector is very nearly aligned with that of the earth's field such that

TABLE IV

Values of induced magnetization (Ji), magnetic susceptibility (K), remanent magnetic intensity (Jr), angle of remanent vector inclination (Ir), and Koenigsberger ratio (Q). [Leader (-) indicates no measurement possible]

Sample depth in feet (meters)	Ji Amp/m	$K \times 10^3$ in SI units	Jr Amp/m	Ir Degrees	(Q)
58 (17.7)	0.18	4.37	1.20	-43	6.6
102 (31.1)	0.18	4.44	1.20	-37	6.5
153 (46.7)	0.18	4.46	2.04	-41	11.1
187 (57.0)	0.024	0.58	0.84	-43	35.0
202 (61.6)	0.24	5.71	3.49	-35	14.8
212 (64.6)	-	-	-	-	-
234 (71.3)	0.098	2.37	0.94		9.6
263 (80.2)	-	-	-	-	-
273 (83.2)	-	-	-	-	-
328 (100.0)	0.13	3.13	0.52	43	4.0
360 (109.8)	0.20	4.81	0.58	50	2.9
421 (128.4)	0.22	5.31	0.39	40	1.8
471 (143.6)	0.064	1.54	0.54	36	8.5
524 (159.8)	0.057	1.37	0.39	48	6.9
569 (173.5)	-	-	-	-	-
623 (189.9)	0.11	2.71	0.91	43	8.1
660 (201.2)	0.067	1.62	0.43	33	6.4
733 (223.5)	0.31	7.38	0.36	49	1.2
772 (235.4)	0.14	3.38	1.07	56	7.7
816 (248.8)	0.24	5.90	0.90	60	3.7
866 (264.0)	0.19	4.69	1.23	53	6.3
921 (280.8)	0.19	4.52	2.1	43	11.2
969 (295.4)	-	-	-	-	-
1010 (307.9)	0.17	4.5	2.9	43	16.9
1040 (317.1)	0.16	3.88	2.41	60	15.0
1112 (339.0)	0.23	5.58	1.86	58	8.1
1183 (360.7)	0.22	5.25	4.23	59	19.5
1249 (380.8)	0.21	4.97	2.08	66	10.1

TABLE IV (con't)

Sample depth in feet (meters)	Ji Amp/m	$Kx10^3$ in SI units	Jr Amp/m	Ir Degrees	(Q)
1266 (386.0)	0.24	5.87	2.59	64	10.7
1304 (397.6)	0.28	6.85	0.94	68	3.3
1324 (403.7)	-	-	-	-	-
1338 (407.9)	-	-	-	-	-
1349 (411.3)	-	-	-	-	-
1361 (414.9)	0.068	1.65	0.084	-	1.2
1411 (430.2)	-	-	-	-	-
1464 (446.3)	-	-	-	-	-
1516 (462.2)	0.014	0.33	0.017	60	1.2
1568 (478.1)	0.011	0.27	0.034	77	3.0
1638 (499.4)	0.036	0.87	0.075	40	2.1
1686 (514.0)	-	-	-	-	-
1741 (530.8)	0.028	0.67	0.061	69	2.2
1791 (546.0)	0.010	0.25	0.077	83	7.4
1833 (558.8)	-	-	-	-	-
1842 (561.6)	0.073	1.77	1.0	40	13.7
1888 (575.6)	0.013	0.31	0.067	48	5.2
1942 (592.1)	0.057	1.38	0.18	73	3.2
1988 (606.1)	0.043	1.04	0.11	78	2.6
2032 (619.5)	0.014	0.35	0.074	62	5.1
2078 (633.5)	0.045	1.08	0.078	69	1.7
2108 (642.7)	0.053	1.27	0.028	66	0.53
2149 (655.2)	-	-	-	-	-
2159 (658.2)	0.086	2.08	0.14	68	1.6
2201 (671.0)	0.095	2.29	0.18	51	1.9
2247 (685.1)	-	-	-	-	-
2300 (701.2)	-	-	-	-	-
2331 (710.7)	-	-	-	-	-
2377 (724.7)	0.018	0.44	0.18	41	9.9
2440 (743.9)	0.017	0.40	0.29	38	17.5
2495 (760.7)	0.006	0.15	0.049	38	7.9

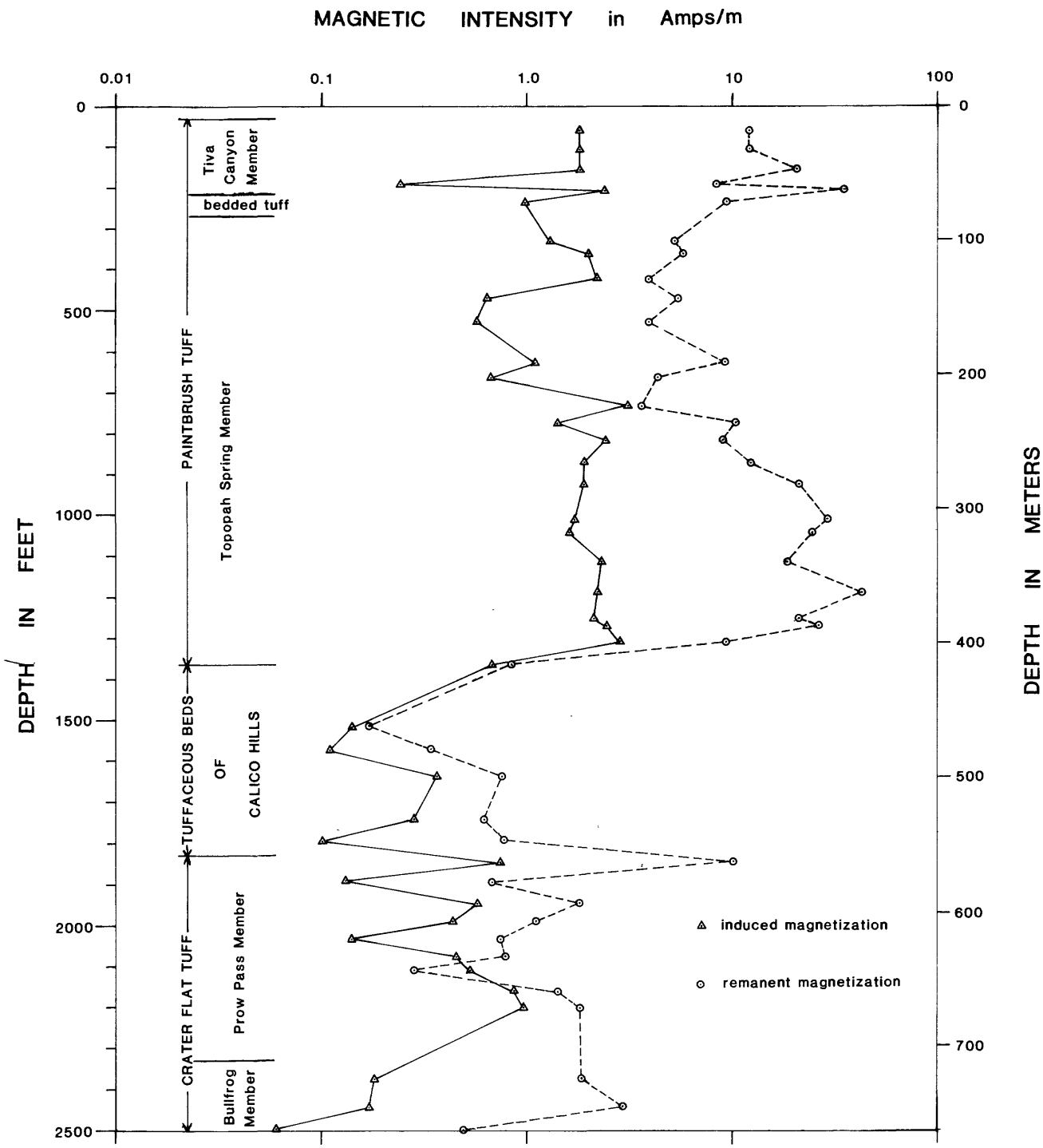

Figure 9- Remanent and induced magnetic intensities of borehole samples plotted with respect to depth of origin. The solid line connects values of remanent magnetization to show variation as a function of depth and is not intended to imply continuity between data points.

both components of magnetization are additive. In contrast, the near surface Tiva Canyon Member has a relatively high magnetic intensity, large Q ratios, and an inversely polarized remanent component sufficient to produce a complex magnetic configuration as mapped at the surface (Gordon Bath, oral communication, 1981).

Summary

Comparisons of resistivity and bulk density measurements made on natural-state and resaturated core samples of tuffs from the NTS-Yucca Mountain borehole indicate that the natural-state rocks are partially desaturated. This holds true for those samples taken from above and below the static water level of the drillhole, suggesting that some pore water loss has taken place during the interim period between removal from the borehole and time of preservation with a beeswax coating. Except for the poorly compacted ash-flow and ash-fall tuff beds and the cavity-filled tuff section of the upper Topopah Spring Member, there is, however, not a great deal of difference in the bulk densities and resistivities of the natural and resaturated samples. The differences between like data sets below the static water level at 469.5 meters (1540 feet) where the rock is expected to be fully water saturated is approximately the same as for those samples taken from above the water table. Water loss through evaporation is therefore believed to have occurred uniformly throughout the rock column, except as noted above, suggesting that those values for saturated rock most nearly approximate the true in situ values.

The patterns of variation noted on the plots of density, resistivity, and compressional sonic velocity is notably similar to that of the porosity plot demonstrating the overall dependence of the indicated rock properties on textural rather than on compositonal changes within the rock. Water accessible porosity varies from a low of 6.0 percent for densely welded tuff to almost

53 percent for the poorly compacted bedded tuffs at the base of the Tiva Canyon Member. The tuffs of the Calico Hills and the Crater Flat Tuff have an average porosity in excess of 20 percent but despite these high porosity values, their permeability to water can be surprisingly low. Much of the low permeability can be attributed to the fine-grained nature of the tuffs and the apparent redistribution of unattached mineral grains within the pore spaces which tends to create an impediment to water flow. No rock subjected to a sustained hydraulic gradient proved to be totally impermeable.

The magnetization of the Paintbrush Tuff is substantially greater than that of the underlying formations and is a potential source of local magnetic anomalies. Remanent magnetization is the principal component of magnetization, and, in the Tiva Canyon Member, the remanent direction is inversely oriented relative to the present-day earth's field. The near surface proximity of the Tiva Canyon Member coupled with its fairly intense and reversed remanent component of magnetization is likely to have an influential and perhaps complicating effect on the surface magnetic field distribution.

The magnetic minerals in the Paintbrush Tuff do not produce an anomalous IP response. Perhaps this is a result of very small grain size or possibly an oxide rind coats the magnetic minerals causing an increase in the surface impedance of the particles such that the polarizing current is diverted through the less resistive pore network of the rock.

References Cited

Chleborad, A. F., Powers, P. S., and Farrow, R. A., 1975; A technique for measuring bulk volume of rock materials: Assoc. Eng. Geologists Bull., v. 12, no. 4, p. 307-312.

Johnson, G. R., 1979, Textural properties, in Hunt, G. R., Johnson, G. R., Olhoeft, G. R., Watson, D. E., and Watson, K., Initial report of the petrophysics laboratory: U.S. Geological Survey Circular 789, pp 67-74.

Mayper, V., 1959, The normal effect-- Parts I and II, in Wait, J. R. Editor, Overvoltage research and geophysical applications: Pergamon Press Inc., New York, London, Paris, pp. 125-158.

Obert, Leonard, and Duvall, Wilbur I., 1967, Rock mechanics and the design of structures in rock: John Wiley and Sons, Inc., New York, London, Sydney, pp. 344-350.

Olhoeft, G. R., Reynolds, R., Friedman, J. D., Johnson, G. R., and Hunt, G. R., 1981, Physical properties of the June 1980 dacite dome at Mount St. Helens: U.S. Geological Survey Prof. Paper, in press.

Pirson, S. J., 1963, Handbook of well log analysis: Prentice-Hall Inc., Englewood Cliffs, New Jersey, 326 p.

Spengler, R. W., Muller, D. C., and Livermore, R. B., 1979, Preliminary report on the geology and geophysics of Drillhole UE25a-1, Yucca Mountain, Nevada Test Site: U.S. Geological Survey Open-File Report 79-1244, 43 p.

Spengler, R. W., and Rosenbaum, J. G., 1980, Preliminary interpretations of geologic results obtained from boreholes UE25a-4, -5, -6, and -7, Yucca Mountain, Nevada Test Site: U.S. Geological Survey Open-File Report 80-929, 33 p.

Sumner, J. S., 1976, Principles of induced polarization for geophysical exploration: Elsevier Scientific Publishing Co., Amsterdam, Oxford, New York, 277 p.

References Cited con't

Watson, D. E., 1979, Magnetic properties, in Hunt, G. R., Johnson, G. R., Olhoeft, G. R., Watson, D. E. and Watson, K., Initial report of the petrophysics laboratory: U.S. Geological Survey Circular 789, pp. 26-49.

GPO 833-820